

## INVESTIGATION OF IONIC SHOCK WAVES IN A COLLISIONLESS PLASMA

S. G. ALIKHANOV, V. G. BELAN, G. N. KICHIGIN, and P. Z. CHEBOTAEV

Nuclear Physics Institute, Siberian Division, USSR Academy of Sciences

Submitted July 29, 1970

Zh. Eksp. Teor. Fiz. 60, 982-992 (March, 1971)

The problem of propagation of a stationary shock wave in a collisionless plasma with thermal ions ( $T_i \neq 0$ ) in the absence of a magnetic field is solved. The dependence of the shock wave velocity on the potential is found for temperature ratios  $T_e/T_i = 10^1-10^3$ . The minimal value  $T_e/T_i = 5$  for which the waves can exist is found. Results of experiments on the propagation of finite-amplitude ionic shock waves in a laboratory plasma ( $T_e/T_i = 20-50$ ) are presented. The initial stage of wave formation and the dynamics of ion reflection from the wave front are studied. The ion distribution function in a plasma is measured for waves with different amplitudes and velocities. Evolution of a large-amplitude wave under conditions close to those in the experiment is studied by carrying out a numerical experiment with a "computer plasma." The results of the theoretical analysis are compared with the experimental data. In all cases considered, the calculations and experiments indicate that the Mach numbers do not exceed 1.6.

## 1. INTRODUCTION

AS is well known<sup>[1-3]</sup>, ion-acoustic waves of small amplitude can propagate in a rarefied plasma with hot electrons ( $T_e \gg T_i$ , where  $T_{e,i}$ —electron and ion temperatures). Great interest attaches to the nonlinear dynamics of propagation of such waves with finite amplitude, especially because a non-isothermal plasma is an example of a strongly dispersive medium with small absorption. As follows from hydrodynamic theory ( $T_i = 0$ ), propagation of nonlinear stable elementary waves, for example compression solitons<sup>[4-6]</sup> is possible in such a medium, and any initial perturbation, generally speaking, breaks up in the course of time into an aggregate of such elementary oscillations with a spatial dimension on the order of the characteristic dispersion length (Debye radius,  $\lambda_D = \sqrt{T_e/(4\pi n e^2)}$ , in this case). The characteristic velocity  $u$  of the collisionless shock wave produced in this manner is of the order of the velocity of ion sound  $v_S = \sqrt{T_e/m_i}$ . For Mach numbers  $M < 1.6$  ( $M = u/v_S$ ), the formation of a sound wave with nonlinear oscillations behind the front has been qualitatively confirmed by numerical calculations<sup>[7,8]</sup> and experimentally<sup>[9,10]</sup>. The hydrodynamic approximation is valid until the amplitude of the potential reaches the critical value  $\varphi_{cr} = 1.3 T_e/e$ <sup>[4]</sup>, above which the "breaking" of the wave takes place and the motion becomes of the two-stream type. As shown in the numerical experiment<sup>[11]</sup>, in which the particle method was used to describe the plasma, at a wave amplitude slightly exceeding the critical value, the "breaking" of the wave as it propagates in a plasma with cold ions ( $T_i = 0$ ) occurs periodically with a frequency  $\sim \omega_{pi}$ . In a real experiment, the ion temperature, while much less than  $T_e$ , remains finite, and there is always a group of ions reflected from the moving potential hump. As follows from<sup>[12,13]</sup>, in this case the structure of the wave can change noticeably.

In the present paper we have investigated the structure of a collisionless shock wave in a plasma with thermal ions. In the first part we find the stationary profile of the potential of the shock wave for different

Mach numbers and ion temperatures ( $T_i/T_e = 10^{-1}-10^{-3}$ ). In the second part we give results of an investigation of the initial stage of motion of a perturbation wave of specified form, as obtained from a numerical experiment. In the third part we describe experiments performed on the "Volna" installation, aimed at the study of the propagation of ionic waves of finite amplitude in a laboratory plasma. It was assumed in the calculations that the distribution of the plasma electrons (including the captured ones) is Maxwellian, and consequently the electron density at any place is described by a Boltzmann distribution. It follows from the results of a comparison of theory and experiment, given in the present paper, that the correctness of this assumption is fully confirmed.

## 2. THEORY AND CALCULATION

Stationary case. To find the profile of the potential in the stationary shock wave for an arbitrary number of reflected particles, it is necessary to solve the Poisson equation

$$d^2\varphi/dx^2 = 4\pi e(n_e - n_i). \quad (1)$$

Here  $n_e$  and  $n_i$  are respectively the densities of the electrons and singly-charged ions,  $e$  is the electron charge, and  $\varphi$  is the electrostatic potential. Let us assume that the density of the electrons at any place is described by a Boltzmann distribution  $n_e = n_0 \exp(e\varphi/T_e)$ , and that there are no captured ions. There is no doubt that the number and the distribution function of the captured ions depend on the method of wave formation. However, if it is assumed that the velocity of the wave greatly exceeds the thermal velocity of the ions, then the number of captured particles will be negligible. To find the solution of Eq. (1) in a form analogous to that obtained in<sup>[12]</sup>, we choose the distribution function of the ions in the unperturbed plasma ( $\varphi = 0$ ) in the form (in a reference frame moving together with the wave)

$$f(v_0) = A \begin{cases} \exp[-m_i(|v_0| - u)^2/2T_i], & v_0 \geq -u, \\ 0 & v_0 < -u, \end{cases} \quad (2)$$

where  $v_0$  is the velocity of the ions in the unperturbed plasma,  $A$  is the normalization factor, and  $w = \sqrt{2e\varphi_A/m_i}$ . Solving the Vlasov stationary equation, we obtain with allowance for (2) the distribution function at any point  $x$ :

$$f(x, v) = A \exp \left[ -\frac{m_i}{2T_i} (\sqrt{v^2 + 2e\varphi(x)/m_i} - u)^2 \right]. \quad (3)$$

Let the coordinate of the maximum of the potential of the frontal wave lie at the point  $x = 0$ . We then assume that in the region  $x > 0$  there fall only those particles from the distribution (2), having a velocity  $v_0 > w$ . When  $x < 0$  the point with arbitrary potential  $\varphi(x)$  is reached by (incoming) particles from (2) with velocities  $v_0 \geq \sqrt{2e\varphi/m_i}$ , and reflected particles lying in the interval  $-w \leq v_0 \leq -\sqrt{2e\varphi/m_i}$ . We thus obtain for the ion density the expressions

$$n(\varphi) = A \left[ \int_0^{\infty} f(\varphi, v) dv + \int_0^x f(\varphi, v) dv \right], \quad x < 0,$$

where

$$n(\varphi) = A \int_x^{\infty} f(\varphi, v) dv, \quad x > 0, \quad (4)$$

$$X = \sqrt{2e(\varphi_A - \varphi)/m_i},$$

and the function  $f(\varphi, v)$  is determined by expression (3). The constant  $A$  is found from the boundary condition at  $x = -\infty$ , where it is assumed that  $\varphi = d\varphi/dx = 0$ ,  $n_i(0) = n_0$ . Consequently,

$$A = n_0 \left\{ \int_0^{\infty} \exp \left[ -\frac{m_i}{2T_i} (u - v)^2 \right] dv + \int_0^{\infty} \exp \left[ -\frac{m_i}{2T_i} (u - v)^2 \right] dv \right\}^{-1}. \quad (5)$$

We choose the dimensionless variables

$$\Phi = e\varphi/T_e, \quad \xi = x/\lambda_D, \quad V = v/u \quad (6)$$

and the notation

$$\Theta = T_e/T_i, \quad p = 2/\Theta M^2, \quad R = 2\Phi/M^2, \quad s = 2\Phi_A/M^2. \quad (7)$$

Substituting (4) with allowance for (5)–(7) into the Poisson equation (1) and integrating once, we obtain

$$\frac{1}{2} \left( \frac{d\Phi}{d\xi} \right)^2 = e^\Phi + BM^2 \left[ \int_{V^*}^{\infty} F(V, R) dV + \int_{V^*}^{\infty} F(V, R) dV \right] + D, \quad x < 0, \quad (8)$$

$$\frac{1}{2} \left( \frac{d\Phi}{d\xi} \right)^2 = e^\Phi + BM^2 \int_{V^*}^{\infty} F(V, R) dV + E, \quad x > 0, \quad (9)$$

where  $F(V, R) = V \sqrt{V^2 - R} \exp[-(V-1)^2/p]$ ,  $B = uA/n_0$ .

The constant  $D$  is found from the boundary condition  $\Phi = d\Phi/d\xi = 0$  ( $x = -\infty$ ), and  $E$  is found from the condition of matching the solutions for the regions  $x < 0$  and  $x > 0$  at  $\Phi = \Phi_A$ :

$$E = D = -1 - \left[ \int_0^{\infty} V^2 \exp[-(V-1)^2/p] dV - \int_0^{V^*} V^2 \exp[-(V-1)^2/p] dV \right] BM^2.$$

In addition, to solve Eqs. (8) and (9) it is necessary to know the relation between  $M$  and  $\Phi_A$  (i.e., between the Mach number and the amplitude of the wave). This relation is obtained from the equation

$$e^{\Phi_A} - 1 = BM^2 \left[ \int_0^{\infty} F(V, 0) dV + \int_0^{\infty} F(V, 0) dV - \int_0^{\infty} F(V, s) dV \right]. \quad (10)$$

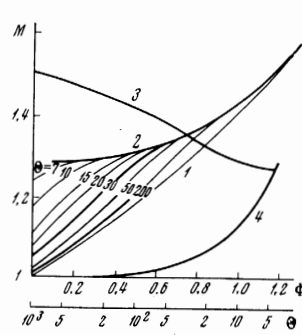


FIG. 1

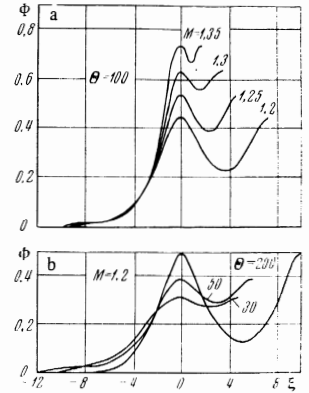


FIG. 2

At low ion temperatures ( $\Theta \gg 1$ ) the integrals in (10) can be determined by expanding the integrand in powers of  $\Theta^{-1}$ . Accurate to terms  $\Theta^{-2}$ , Eq. (10) is written in this case in the form

$$e^{\Phi_A} - 1 = M^2(1 - \sqrt{1-s}) + \frac{1}{2\Theta} [2 - 3(1-s)^{-1/2} + (1-s)^{-3/2}].$$

From this we can obtain the increment to the wave velocity due to the thermal motion:

$$m = \frac{1}{2M_0\Theta} \frac{2(1-s_0)^{1/2} - 3 + (1-s_0)^{-1}}{2-s_0 - 2(1-s_0)^{1/2}}$$

where  $M_0$  is the velocity of the wave at  $\Theta = \infty$ , and  $s_0 = 2\Phi_A/M_0^2$ . At low wave amplitudes, the wave velocity tends to the velocity of the hydrodynamic ion-acoustic wave  $M = \sqrt{1 + 3/\Theta} \approx 1 + 3/2\Theta$ . However, when  $\Phi_A < \exp(-2T_e/T_i)$  expression (1) has no solution. (This circumstance was pointed out to us by A. V. Gurevich.) The reason for it is that when  $\Phi_A \rightarrow 0$  the concentration of the reflected ions is proportional to  $n_{\text{ref}} \sim \sqrt{\Phi_A} \exp(-T_e/T_i)$ , whereas the increase of the ion concentration on the crest of the wave is  $\Delta n_i \sim \Phi_A$ , and therefore when  $\Phi_A < \exp(-2T_e/T_i)$  we have  $n_{\text{ref}} > \Delta n_i$ , and no compression wave is produced. It should be noted that owing to the smallness of  $\exp(-2T_e/T_i)$ , the region where there is no stationary wave is very small and practically merges with the ordinate axis on the scale of Fig. 1.

The results of the solution of Eqs. (8)–(10) are shown in Figs. 1 and 2. The relations between the wave velocity and the amplitude of the potential are shown in Fig. 1. The region of existence of solutions is bounded by the curves 1 and 2. Curve 1 is the plot for hydrodynamic solitary waves (solitons), and curve 2 is the envelope of the limiting values of the Mach numbers. The limiting values are obtained from Eq. (10) with simultaneous satisfaction of the quasineutrality condition:  $n_e(\Phi_A) = n_i(\Phi_A)$  at  $\Phi = \Phi_A$ . In this case the solution has a monotonic character.

At a negligibly low ion temperature  $T_i/T_e = 10^{-3} - 10^{-4}$ , the plot of  $M(\Phi_A)$ , as expected, is close to curve 1. The wave profile at  $M - 1 \ll 1$  can be represented in this case as an aggregate of almost non-interacting solitons, and the form of the frontal soliton practically coincides with the profile of the solitary wave at the same value of  $M$ . This fact makes it possible to represent qualitatively the shock wave as an aggregate of repelling solitons kept in equilibrium on the one side

by a kind of piston producing these solitons, and on the other by the pressure of the reflected particles.

Figure 1 also shows the dependence of the limiting values of the Mach numbers and the velocity of the hydrodynamic ion-acoustic wave on  $\Theta$  (curves 3 and 4, respectively). The point of intersection of the curves gives the critical value of the ion temperature  $T_i \approx 0.2T_e$ , above which the existence of the shock wave is impossible.

Figure 2a shows the profile of the potential of the shock wave at different wave velocities for a fixed value of  $\Theta$ , while Fig. 2b shows the same for different plasma ion temperatures at a given value of  $M$ . It follows from Fig. 2 that the amplitude and period of the oscillations decrease with increasing ion temperature and wave velocity.

The final results obtained in the present study differ somewhat from the results of Bardotti and Segre<sup>[13]</sup> who used a solution method different from that given above. In particular, the dependence of the limiting Mach numbers  $M_N = M_N(\Theta)$  does not coincide with the relation obtained by us from the exact formula (10) (curve 3, Fig. 1), apparently because the approximate method of determining  $M_N$ , given in<sup>[13]</sup>, is quite inaccurate.

**Nonstationary case.** To solve the problem of the evolution of a given perturbation of the density we used the method of numerical experiment with a model plasma. Use of this method permits the closest approach to the conditions of a real experiment. In the one-dimensional case of interest to us, we assume that the electron density has a Boltzmann distribution, and that the ion component of the plasma is represented in the form of an aggregate of a finite number of charged particles, amounting to  $2-7 \times 10^3$  for different variants. The field distribution at any instant of time is determined from Eq. (1). The position of the center of the  $j$ -th particle in space, at a known field distribution, is determined from the equation

$$\frac{dv_j}{dt} = -\frac{e}{m_i} \frac{\partial \varphi}{\partial x}$$

The particles with a specified distribution at the initial instant of time could move in an interval of  $\sim 100$  Debye units. At the limits of the interval  $[0, L]$  the conditions stipulated for the potential were

$$\varphi'(0) = \varphi'(L) = 0 \tag{11}$$

and the particles were reflected on reaching the limit. The solution of the boundary-value problem (1), (11) was obtained by a numerical method similar to that used in<sup>[11]</sup>. In place of (1) we solved the partial differential equation

$$\psi(\varphi) = -\psi'_\varphi \psi'_\varphi, \tag{12}$$

where  $\psi(\varphi) = \varphi_{xx} + 4\pi e [n_i - n_0 \exp(e\varphi/T_e)]$ . The stationary solution of Eq. (12), obtained for  $t \rightarrow \infty$ , serves as a solution of the initial equation (1).

If we denote by  $\varphi_k^m$  the value of the potential at the instant of time  $t^m = m\Delta t$  at a node of the spatial grid  $x_k = k\Delta x$ , then the density of the ions  $n_{ik}^m$  is defined as the number of particles located at the instant of time  $t^m$  between the coordinates  $x_{k-1/2}$  and  $x_{k+1/2}$ , multiplied by the normalization coefficient. To decrease the

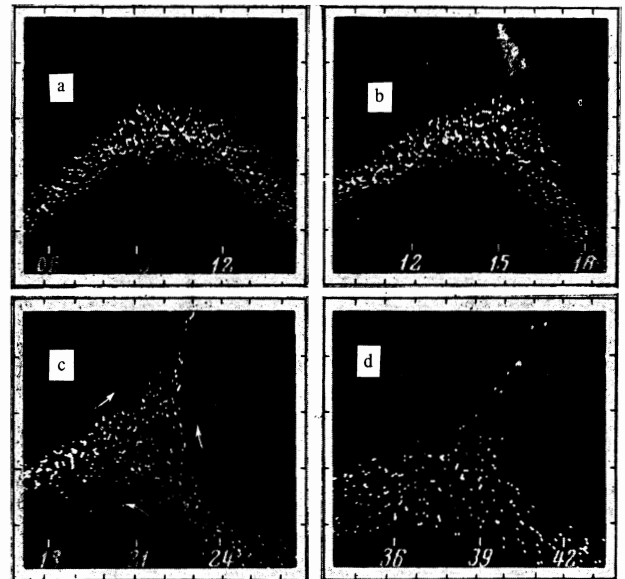


FIG. 3. Phase space. Frames from the film for values of  $t\omega_{pi}$  equal to: a-0, b-2, c-5.4, d-17.

density jumps as the particle passes through the boundaries  $x_{k-1/2}$  and  $x_{k+1/2}$ , the particles were "smeared out" in space, and this led to a certain distortion of the dispersion properties of the plasma<sup>[11]</sup>.

This method was used to determine the motion of an ion-acoustic wave with an initial density profile

$$N(x) = 1 + N_0 \exp[-(x - x_0)^2 / l^2],$$

and a velocity in the form  $v(x) = v_S \ln \{N(x)\}$ , where  $N_0$  is the amplitude of the perturbation and  $l$  is its half-width. In the numerical calculations, the temperature ratio ( $\Theta = 20$ ) and the density drop in the wave ( $N_0 = 3$ ) were taken from calculation of the proximity to experiment with an ionic wave of large amplitude. The thermal noise was set by a random-number generator.

The state of the phase space ( $v, x$ ) was displayed on an oscilloscope screen<sup>[14]</sup>, making it possible to trace the position of each particle in time. Figure 3 shows the state of phase space in the region of the maximum potential of the wave (the  $x$  scale is in units of  $\lambda_D$ , and the  $y$  scale is  $0.5v_S$  per division). A gradual increase of the slope of the wave was observed ( $t = 2\omega_{pi}^{-1}$ ), and starting with a certain time there was observed also a reflection of the particles from the leading front of the wave ( $t = 5.4\omega_{pi}^{-1}$ ). The presence of thermal noise causes only part of the incoming flux to be reflected (in contrast to the case  $T_i = 0$ ). At  $t = 5.4\omega_{pi}^{-1}$  one can see clearly three streams: one accelerated from the crest of the wave, one reflected, and one transmitted.

Figure 4 shows the evolution of the potential of the wave. The small-scale oscillations of the potential are connected with the finite number of particles per Debye radius. The deceleration of the wave, the decrease of its amplitude, and the reflection of the particles occur continuously, and no pulsations were observed in the calculations as in the case of  $T_i = 0$ <sup>[11]</sup>.

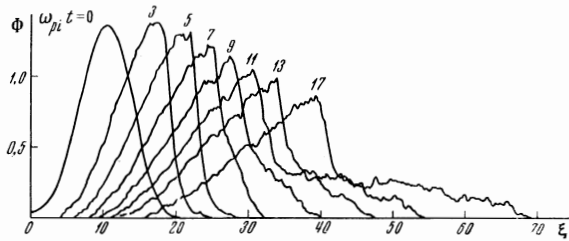


FIG. 4

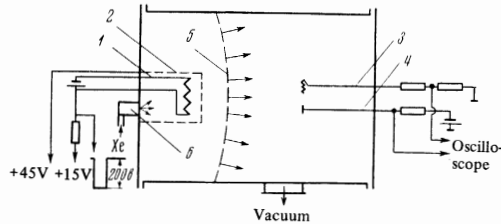


FIG. 5. Experimental setup: 1—incandescent cathode, 2—anode, 3—emission probe, 4—Langmuir probe, 5—profile of gas cloud, 6—pulsed gas valve.

### 3. EXPERIMENT

**Production of plasma.** The schematic diagram of the setup is shown in Fig. 5. A cylindrical vacuum volume (diameter  $\approx 100$  cm,  $l \approx 150$  cm) was evacuated to a pressure  $p \sim 10^{-6}$  mm Hg. Xe gas was injected from the end with the aid of a pulsed gas valve. The expanding gas cloud was ionized by a stream of accelerated electrons from an incandescent cathode placed at a distance  $\sim 10$  cm from the point of injection of the gas. The plasma produced in this manner spreads with a velocity much larger than the velocity of motion of the neutral gas. The rate of flow of the neutral gas is  $4 \times 10^4$  cm/sec. The average plasma flow velocity is  $4 \times 10^5$  cm/sec. After a time  $\sim 1$  msec, a quasistationary flow of the plasma is established. In that time interval the plasma parameters do not vary in time along the axis of the volume. The potential decreases along the axis; the ions produced in the part of the volume occupied by the gas are accelerated in such a way that at the opposite end of the volume their velocity reaches  $5 \times 10^5$  cm/sec ( $2M$ ). At some instant of time, when the neutral gas occupies approximately one quarter of the volume, a negative pulse of rectangular form, of duration 5–40  $\mu$ sec, is applied to the cathode. This increases the flow of electrons from the cathode and the degree of ionization of the neutral gas. By varying the amplitude and duration of the pulse it is possible to vary the size of the density drop. The spatial dimension of the front of the initial perturbation of the density is  $\sim 10$  cm. The plasma density drop produced in this manner approximately duplicates the profile of the neutral gas.

**Diagnostics.** The density of the plasma and the temperature of the electrons were determined from the electronic part of the probe characteristic, plotted after a time 10  $\mu$ sec. By differentiating this characteristic twice, it is possible to obtain the electron distribution function, which in these experiments was close to Maxwellian. Typical plasma parameters are  $T_e \approx 5-7$  eV,  $n_e \approx 3 \times 10^7$  cm $^{-3}$ , the mean free path of the

electrons and ions is determined by the collisions with the neutral particles and amounts to  $\sim 10^3$  cm.

The time variation of the ion density was registered with the aid of single probes operating in the ion saturation current mode. Since the stream velocity was large compared with the change of the particle velocity in the wave, the increase of the probe current is proportional to the ion density.

The particle spectrum was measured with an ion-velocity time-of-flight analyzer. The open time of the analyzer shutter, which formed a narrow packet of ions from the investigated region of the plasma, was chosen to be 0.5  $\mu$ sec, which is much less than the characteristic time of variation of the potential in the wave ( $\approx 5$   $\mu$ sec). At a flight-tube length 22 cm, the analyzer ensured a resolution of about 5% in a velocity interval  $8 \times 10^5 - 1.2 \times 10^6$  cm/sec. The potential of the plasma was measured by an incandescent probe. Owing to the relatively low resistance of the plasma-probe contact and the high resistance of the output divider, the probe potential was close to the plasma potential. The probe filament supply circuit was turned off during the measurement time, and the capacitance of the filament to ground was 1–2 pF. This made it possible to obtain a time resolution of 0.2  $\mu$ sec.

The velocity of the wave was determined from the time shift of the signals from two probes shifted relative to one another along the direction of propagation of the wave. In addition, by measuring the amplitude of the potential in the wave and the shift of the maximum of the distribution function  $\Delta M$ , the wave velocity  $M$  can be calculated from the expression

$$\Delta M = M - \sqrt{M^2 - 2\Phi_A}$$

**Ion spectrum in plasma stream.** Since the plasma potential decreases with increasing distance from the point of injection of the gas, the production of ions as a result of ionization occurs at points with different potentials. This leads to a scatter of the energy spectrum of the ions in the stream. Depending on the potential difference on the boundaries of the region in which the ions are produced, the width of the energy spectrum of the particles in the plasma stream varies. Thus, by varying the dimension of the gas cloud it is possible to vary the energy scatter of the plasma ions in a certain range.

The energy spectrum of the ions was close to Maxwellian, so that it is meaningful to speak of an ion temperature. The ion temperature in the stream system  $T_i$  can be determined from the expression

$$\Delta \epsilon = 2\sqrt{T_i \epsilon_0} + T_i,$$

i.e., in comparison with the energy scatter in the laboratory coordinate system  $\Delta \epsilon$ , which is measured with the analyzer,  $T_i$  in the stream is smaller by a factor  $\Delta \epsilon / 4\epsilon_0$  (for  $\Delta \epsilon \ll 4\epsilon_0$ ); here  $\epsilon_0 = m_i V_0^2 / 2$ , where  $V_0$  is the average stream velocity. The stream velocity was determined from the propagation velocity of the small-amplitude wave under the assumption that the velocity of such a wave in the stream system is close to  $v_S$ . In addition,  $\epsilon_0$  can be determined if one knows the potential and the total energy of the ions measured by the analyzer.

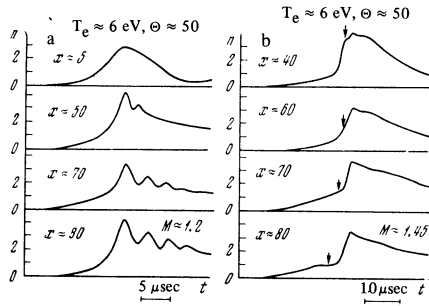


FIG. 6

In these experiments, the energy scatter  $\Delta\epsilon$  for different cases was varied in the range 2.5–4.5 eV, corresponding to an ion temperature in the stream  $T_i = 0.1\text{--}0.3$  eV at  $\epsilon_0 \approx 16$  eV.

**Results of experiments and discussion.** Figure 6a shows oscillograms of the profile of  $n$ , illustrating the evolution of the wave as a function of the distance traversed by the wave for  $M = 1.2$  (the wave velocity was determined at  $x = 80$  cm).  $n$  is given in arbitrary units. As the wave advances, the initially smooth perturbation becomes steeper, and oscillations appear behind the wave; their amplitude increases with increasing distance traversed by the wave, and the width of the wave front, starting with a certain instant, remains constant. As follows from the experiments, the initial perturbation breaks up into elementary oscillations with a characteristic dimension on the order of  $\lambda_D$ . Starting with a certain distance ( $x = 70$ ), owing to the presence of a small number of reflected particles, a quasistationary motion is established. The wavelength of the oscillations, equal to approximately  $6\text{--}7\lambda_D$ , approximately coincides with the calculated one obtained for the stationary case for the same values of  $M$  and  $\Theta$  (Fig. 2).

Figure 6b shows profiles of  $n$  in the case of a large-amplitude wave ( $M = 1.45$ ,  $\Theta \approx 50$ ). The arrows denote the positions of the particles accelerated in the front of the wave. The profile of such a wave differs significantly from the profile of a small-amplitude wave. First, the increase of the slope occurs at shorter distances; second, there are no clearly pronounced periodic oscillations behind the front, and ahead of the front there appear fast ions, which drift forward and form pedestal waves. These can include both particles reflected from the front and those rolling over the crest of the wave, but they cannot be distinguished experimentally. As follows from numerical calculations, where analogous processes were observed, the main contribution is made by the reflected particles.

Figure 7 shows profiles of  $n$  and  $\phi$  at different Mach numbers ( $\Theta = 50$ ). We see that with increasing wave velocity the amplitude of the potential increases, the period and the depth of the oscillations decrease, and the slope of the front increases somewhat. In the presence of an appreciable number of reflected particles, there are practically no oscillations on the profile of the wave ( $M = 1.45$ ).

With increasing ion temperature ( $\Theta = 20$ , Fig. 7), the amplitude and period of the oscillation are much smaller for the same Mach numbers.

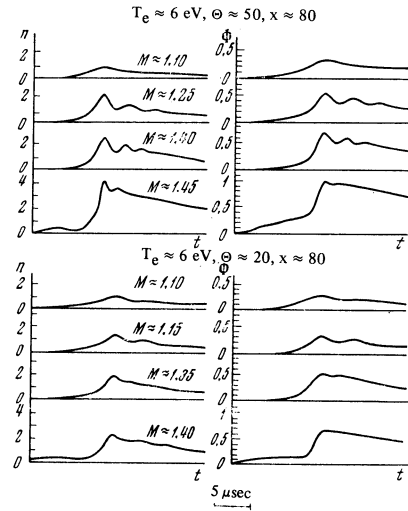


FIG. 7

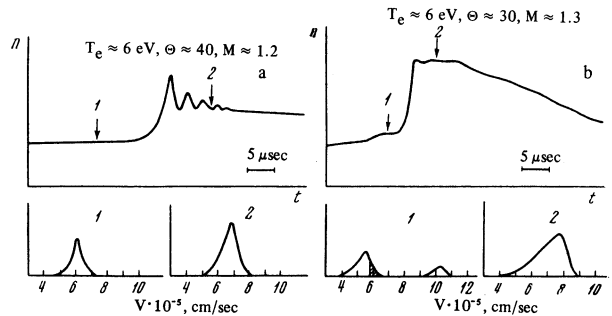


FIG. 8

The experimental results shown in Fig. 7 are in qualitative agreement with the calculations for a stationary shock wave (Fig. 2). As follows from the calculation (Fig. 1), at  $\Theta = 50$  and  $\Theta = 20$  the limiting wave velocities are respectively  $M \approx 1.4$  and  $M \approx 1.3$ . Approximately the same values were obtained in the experiment, but with further increase of the amplitude of the initial perturbations the wave velocity increases slowly. This can be attributed to the fact that as the number of the ions reflected by the wave increases, the potential  $\Phi_0$  ahead of the front of the wave increases greatly, leading to an increase of the limiting amplitude of the potential of the wave to a value  $\Phi_{CR} \approx (M^2 + \Phi_0)/2$ . In the case of small  $M$ , when  $\Phi_0 \approx 0$ , the amplitude of the potential, as follows from Fig. 7, is close to the calculated one for a stationary wave.

Particular interest attaches to an investigation of the ion velocity distribution function at different points of the wave profile. In each experiment, as a rule, the spectrum was investigated at two points of space; ahead of the front and behind the front of the wave. Simultaneously with this, the potential and wave velocity were measured.

Figure 8a shows the spectrum of the ions ahead of the wave (1) and behind the front of the wave (2) for the case of a small number of reflected ions ( $M = 1.2$ ). Behind the front, the maximum is shifted towards larger velocities, and broadening of the spectrum is observed. This form of the distribution function of the

ions in the wave of the potential agrees qualitatively with the function described by formula (3). The distribution of the particles in the plasma after the passage of the wave (at the point  $\varphi \approx 0$ ) hardly differs from the unperturbed distribution.

Figure 8b shows the distribution function of the particles ahead of the wave and behind the front of the wave of large amplitude. Behind the front of the wave (2) in the region of large velocities, the spectrum is cut off, and ahead of the front (1) there appeared a group of reflected particles. Since all the particles whose velocities (in the laboratory frame) exceed a certain limiting value are reflected (the shaded part of the spectrum of the unperturbed plasma), it follows that the spectrum of the reflected particles is smeared out. If the reflection process has a stationary character, then the spectrum should decrease abruptly at a certain velocity. The form of the spectrum behind the wave front (2) coincides, in the main, with the calculated one. As seen from the phase picture (Fig. 3d,  $t = 17\omega_{pi}^{-1}$ ) and from the experimental data (Fig. 8b (2)), the spectrum is strongly smeared out in the region of low velocities and decreases quite sharply at a velocity approximately equal to the wave velocity.

The smearing of the experimental spectrum behind the wave front and of the spectrum of the fast particles ahead of the wave front in the region of large velocities is much more appreciable than could be caused by the resolution of the analyzer. This can be attributed to the nonstationary character of the reflection process.

In conclusion, the authors are deeply grateful to R. Z. Sagdeev for constant interest in the work and for valuable advice.

- <sup>1</sup>L. Tonks and I. Langmuir, *Phys. Rev.*, **33**, 195 (1929).
- <sup>2</sup>I. Alexeff and R. V. Neidigh, *Phys. Rev.*, **129**, 516 (1963).
- <sup>3</sup>I. Alexeff and W. D. Jones, *Phys. Rev. Lett.*, **15**, 286 (1965).
- <sup>4</sup>R. Z. Sagdeev, in *Voprosy teorii plazmy* (Problems of Plasma Theory) V. 4, Gosatomizdat, 1964, p. 20.
- <sup>5</sup>V. I. Karpman, *Phys. Lett.*, **25a**, 708 (1967).
- <sup>6</sup>C. S. Gardner, J. M. Greene, M. D. Kruskal, and R. M. Miura, *Phys. Rev. Lett.*, **19**, 1095 (1967).
- <sup>7</sup>D. Biskamp, K. L. Lackner, and D. Parkinson, *Proc. of Third European Conf. on Contr. Fusion and Plasma Phys.*, Utrecht, The Netherlands, 23–27 June, 1965.
- <sup>8</sup>R. J. Mason, *Phys. Fluids*, **13**, 1042 (1970).
- <sup>9</sup>S. G. Alikhanov, V. G. Belan, and R. Z. Sagdeev, *ZhETF Pis. Red.* **7**, 405 (1968) [*JETP Lett.* **7**, 318 (1968)].
- <sup>10</sup>R. J. Taylor, D. R. Baker, and M. Ikezi, *Phys. Rev. Lett.*, **24**, 206 (1970).
- <sup>11</sup>S. G. Alikhanov, R. Z. Sagdeev and P. Z. Chebotaev, *Zh. Eksp. Teor. Fiz.* **57**, 1565 (1969) [*Sov. Phys.-JETP* **30**, 847 (1970)].
- <sup>12</sup>S. S. Moiseev and R. Z. Sagdeev, *Plasma Phys.* (*J. Nucl. Energy*, part C), **5**, 43 (1970).
- <sup>13</sup>G. Bardotti and S. E. Segre, *Plasma Phys.* **12**, 247 (1969).
- <sup>14</sup>V. A. Alekseev and V. A. L'vov, in *Vychislitel'nye sistemy* (Computer Systems), No. 35, 1969.

Translated by J. G. Adashko